

Article

# Comparison of Different Methods for Evaluating Quantitative X-ray Fluorescence Data in Copper-Based Artefacts

Eleni Konstantakopoulou <sup>1,\*</sup>, Annalaura Casanova Municchia <sup>2,\*</sup> , Loredana Luvidi <sup>2</sup> and Marco Ferretti <sup>2</sup> <sup>1</sup> Polytechnic School, Aristotle University of Thessaloniki (AUTH), 54124 Thessaloniki, Greece<sup>2</sup> Institute of Heritage Science (CNR-ISPC), National Research Council of Italy, Area della Ricerca di Roma 1, Montelibretti, Via Salaria Km 29,300, 00010 Rome, Italy; loredana.luvidi@cnr.it (L.L.); marco.ferretti@cnr.it (M.F.)

\* Correspondence: konstantakopoulou\_e@hotmail.com (E.K.); annalaura.casanovamunicchia@cnr.it (A.C.M.)

**Abstract:** Handheld X-ray Fluorescence devices (HH-XRF) have given archaeologists and conservators the opportunity to study a wide range of materials encountered in their work with great accessibility and flexibility. The investigation of copper-based artefacts is a frequent application of these instruments in the field of cultural heritage as it gives direct and rapid quantitative results that can provide very important information about them, such as their fabrication technology. This paper discusses the comparison of quantitative results, obtained by a commercial handheld XRF device “Bruker Tracer 5g” on certified standards, compositionally significant in copper-based alloys of interest in the field of cultural heritage. The measured elemental concentrations were derived using three different calibrations, which were examined for their accuracy. Two of them were based on the empirical coefficients approach, performed by the built-in calibration/software (copper alloy calibrations provided by Bruker manufacturer and the Bruker EasyCal software), while the third one was performed off-line by processing the spectra with an independent fundamental parameters (FP) software (PyMca version 5.9.2., a X-ray fluorescence analysis software developed at the European Synchrotron Radiation Facility). The results highlight that although HH-XRF devices simplify data collection, for optimal quantitative results, the correct choice of analysis conditions and calibration method still requires a detailed understanding of the principles of X-ray spectrometry.

**Keywords:** handheld XRF; calibration; quantitative analysis; copper alloys; cultural heritage



**Citation:** Konstantakopoulou, E.; Casanova Municchia, A.; Luvidi, L.; Ferretti, M. Comparison of Different Methods for Evaluating Quantitative X-ray Fluorescence Data in Copper-Based Artefacts. *Condens. Matter* **2024**, *9*, 5. <https://doi.org/10.3390/condmat9010005>

Academic Editors: Alessandro Scordo and Fabrizio Napolitano

Received: 13 November 2023

Revised: 28 December 2023

Accepted: 10 January 2024

Published: 11 January 2024



**Copyright:** © 2024 by the authors. Licensee MDPI, Basel, Switzerland. This article is an open access article distributed under the terms and conditions of the Creative Commons Attribution (CC BY) license (<https://creativecommons.org/licenses/by/4.0/>).

## 1. Introduction

X-ray fluorescence (XRF) spectrometry is used as one of many analytical techniques to explain the human past in twenty-first century archaeology [1]. The non-destructive capabilities of XRF are indeed particularly suited to research in the field of cultural heritage, where the sample is unique or its integrity has significant technical or esthetic value [2]. In recent decades, technological developments in X-ray generation and detection have led to the production and commercialization of different types of portable instruments [3], with the most widely used being the so-called hand-held XRF devices (HH-XRF) [4]. These instruments are characterized by highly miniaturized hardware and powerful software and are capable of qualitative and quantitative in situ analysis, which make them suitable for work inside museums and conservation laboratories for the characterization of a wide range of cultural heritage objects.

X-ray fluorescence (XRF) analysis by portable spectrometers has long been applied to the study of ancient metals for the identification and characterization of different alloys [5,6]. A large category of metal objects that exist in museums but also in the field are copper-based artefacts, which range from small tools to large-scale statues. Many studies have been carried out concerning the analysis of ancient and historic copper alloys using portable XRF spectrometers, including HH-XRF devices [7–12]. The quantitative results provided

by XRF measurements in a copper-based artefact are very important because the alloy's composition can provide researchers in the field of cultural heritage information about the artefact's authenticity and fabrication technology.

Quantitative XRF analysis consists of converting the measured intensities of the characteristic radiation into the concentrations of the analyzed elements [13]. Nowadays, two calibration methods are commonly used: empirical calibration and the fundamental parameters (FP) approach [14–16].

Empirical calibration requires the use of several standards, whose matrix characteristics are as close as possible to that of the unknown samples. In detail, it relies on algebraic equations that correlate the analyte concentration in a sample with its measured X-ray intensity and the coefficients of such equation are determined by least squares regression [4]. The most common methods in use within the class of empirical calibration are Compton Normalization [17] and Multiple Linear Regression of Lucas Tooth and Price [18,19].

Whereas the fundamental parameters approach is based on the Sherman equation [20], which is later improved by Shiraiwa and Fujino [21], a contemporary FP-based calibration is predicated on a system of exact equations correlating measured intensities of the analytes with their concentrations via the use of fundamental laws, principles, and physical constants governing the interaction of X-rays with matter [22]. Accuracy depends on the uncertainty with which the parameters describe the sample spectrometer system [23–25].

Handheld XRF devices offer different approaches to perform calibration procedures [26]. The most rapid and common method is using a built-in general-purpose calibration of modern alloys, which allows for quick reading of results. However, a question arises regarding the accuracy of quantitative results in applications like studying archaeological copper-based artifacts and not modern one. Otherwise, additional calibration software based on empirical coefficients or the FP approach are used. To perform these calibrations, several standards are needed and need to be as close as possible to that of the unknown samples.

Obtaining appropriate standards for XRF analysis of cultural heritage material can be complex, particularly in the case of copper archaeological ancient material due to the wide range of concentrations found in heritage copper alloys [27]. However, in 2010, a new set of certified reference materials (CRMs) was developed to assist scientists and conservators working in cultural heritage fields with quantitative X-ray fluorescence (XRF) analysis of historical and prehistoric copper alloys [27]. This set of CRMs is known as the Copper CHARM Set (Cultural Heritage Alloy Reference Material Set).

The HH-XRF devices feature a user-friendly design that can sometimes lead archaeologists and conservators to view them as “black boxes” without considering some complex aspects of the calibration and proceeding independently for the material characterization [26]. However, this perception can be problematic in interpreting quantitative XRF data accurately.

For this purpose, this research aims to compare various calibration methods used for HH-XRF devices to perform more accurate quantitative X-ray fluorescence analysis. The final goal is to provide guidance to operators on how to perform proper instrument set-up and calibration before analyzing historical copper alloys. By highlighting the limitations of built-in calibrations and the importance of selecting appropriate voltage for excitation of elements, this study can aid in improving the accuracy of quantitative analysis in the field of archaeometry.

In detail, this paper evaluates the quantitative results obtained by a commercial HH-XRF, i.e., Bruker Tracer 5, on 26 copper-based standards and using three different calibration procedures. Two of them are based on the empirical coefficients approach, performed by the built-in software. One was provided by Bruker with the instrument, whereas the other was a customized calibration that we implemented following the Bruker procedure. The third calibration was performed off-line by processing the spectra with the fundamental parameters software PyMCA (version 5.9.2) [28].

## 2. Results

The XRF spectrum of the certified reference material B21 is reported in Figure 1 as an example of the spectra acquired on the 26 standards. The spectrum highlights the characteristic lines of its alloying constituent elements.

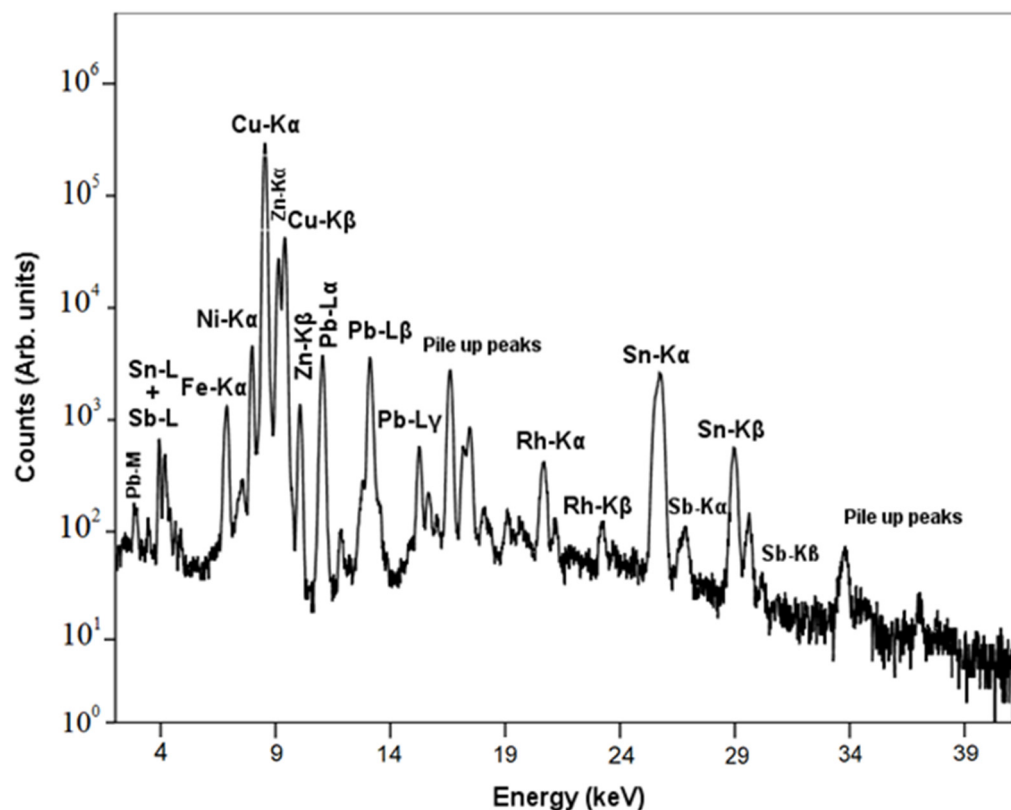


**Figure 1.** XRF spectrum of the certified reference material B21 derived from Bruker Tracer 5g. The characteristic emission lines in XRF spectrum are presented in logarithmic scale.

The R squared and Root Mean Squared Error (RMSE) values obtained from Linear Regression Analysis on the elements present in copper-based cultural heritage alloys are summarized in Table 1. Based on the results, the Pymca and Customized Bruker methods show more accurate calibration, closest to an R squared value of 1 and at the same time to the lowest RMSE value, compared to the Bruker Built-in method. Specifically, for elements such as Mn, Fe, Ni, and As, the Pymca approach is the most accurate, while for elements such as Ag, Cd, Pb, and Bi, the Customized Bruker method provides the best results. Finally, for elements such as Co, Zn, Ag, Sn, and Sb, both methods show an accurate calibration.

Figures 2 and 3 display quantitative results obtained from the three different calibrations for Tin (Sn) and Antimony (Sb), high-Z elements representative and relevant for studying copper materials. In detail, the graphs (Figures 2 and 3) indicate that the Linear Regression Line of the Bruker Built-in Calibration has a bias from the bisector. This suggests the presence of systematically positive deviations from the nominal concentration values, which means a poor calibration performance. However, we observe minimal deviations in the calibrated concentrations of Sn and Sb in both Off-Line PyMca and Customized Bruker compared to the Built-in Calibration.

**Table 1.** R<sup>2</sup> squared and RMSE values obtained from Linear Regression Analysis.

Element	Calibration Procedure	R <sup>2</sup>	RMSE
Mn	Off-Line PyMca	0.998	0.007
	Customized Bruker	0.953	0.031
	Bruker Built-in	0.926	0.029
Fe	Off-Line PyMca	0.996	0.015
	Customized Bruker	0.982	0.034
	Bruker Built-in	0.860	0.092
Co	Off-Line PyMca	0.998	0.008
	Customized Bruker	0.999	0.005
	Bruker Built-in	0.974	0.041
Ni	Off-Line PyMca	0.997	0.021
	Customized Bruker	0.951	0.085
	Bruker Built-in	0.982	0.050
Zn	Off-Line PyMca	1.000	0.189
	Customized Bruker	1.000	0.121
	Bruker Built-in	0.997	0.451
As	Off-Line PyMca	0.996	0.024
	Customized Bruker	0.992	0.031
	Bruker Built-in	0.961	0.079
Ag	Off-Line PyMca	0.997	0.028
	Customized Bruker	1.000	0.012
	Bruker Built-in	0.994	0.048
Cd	Off-Line PyMca	0.983	0.016
	Customized Bruker	0.993	0.012
	Bruker Built-in	0.925	0.045
Sn	Off-Line PyMca	0.999	0.145
	Customized Bruker	0.999	0.122
	Bruker Built-in	0.997	0.251
Sb	Off-Line PyMca	0.999	0.024
	Customized Bruker	0.999	0.025
	Bruker Built-in	0.982	0.149
Pb	Off-Line PyMca	0.991	0.328
	Customized Bruker	0.997	0.217
	Bruker Built-in	0.991	0.386
Bi	Off-Line PyMca	0.986	0.025
	Customized Bruker	0.996	0.017
	Bruker Built-in	0.959	0.049

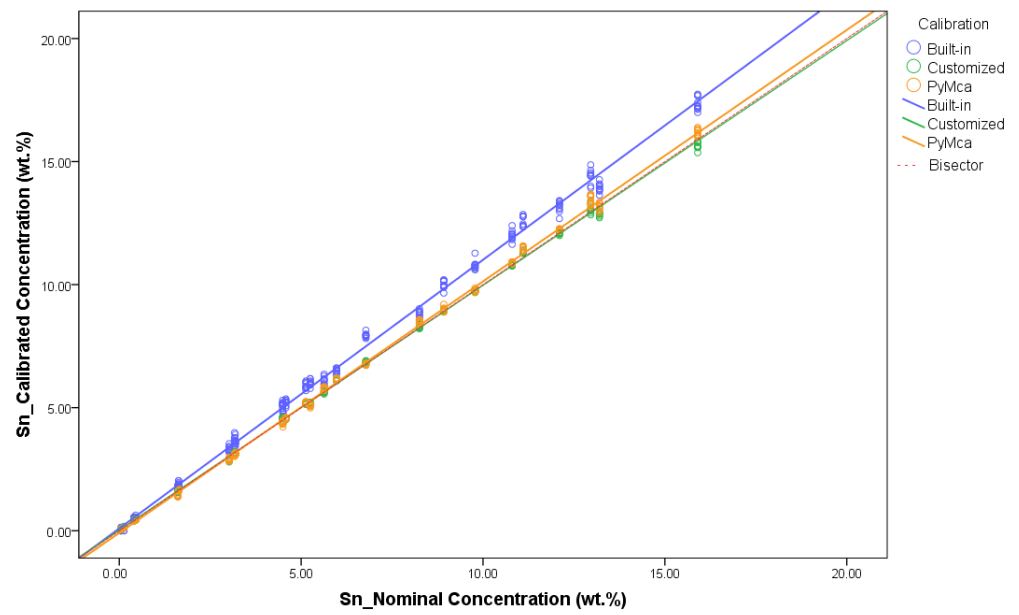


Figure 2. Linear Regression Analysis on Sn and comparison of three calibration procedures.

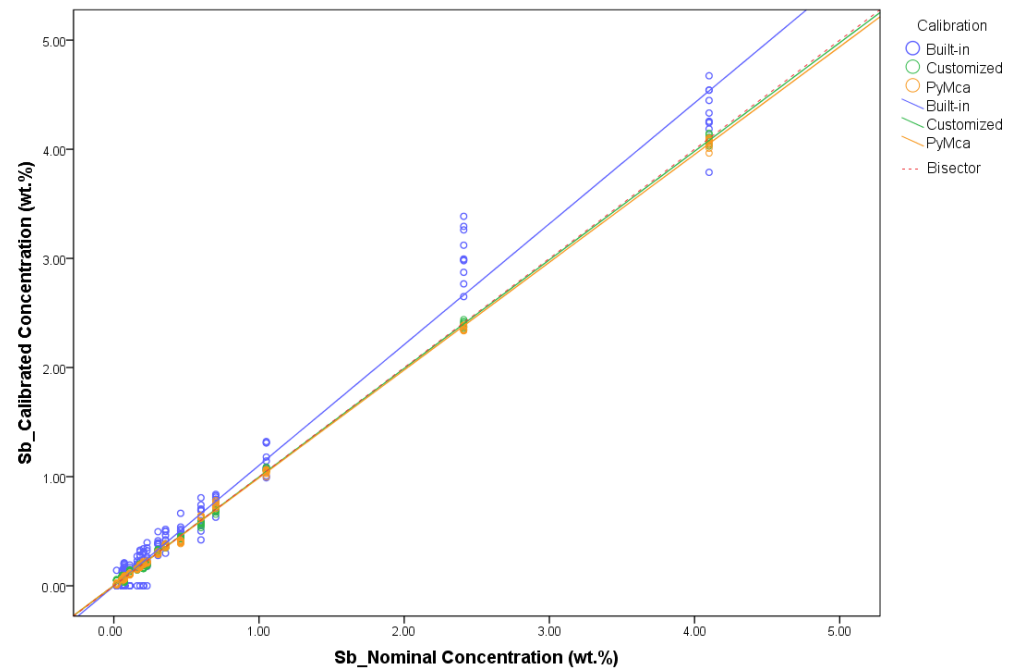


Figure 3. Linear Regression Analysis on Sb and comparison of three calibration procedures.

In Figure 4, the Linear Regression Analysis of Iron (Fe), a low-Z element, is underlined. Here, Iron is considered a low-Z element because it is one of the last detectable elements in copper materials using our XRF configuration. This is accomplished by comparing three calibration procedures. From the results, in this case the Built-in Calibration also has a bad performance, while the other two calibrations have more reliable quantitative results. The same trend is pointed out in Figure 5, which compares the RMSE values between the three different calibration procedures on all elements present in the copper-based alloys. Built-in Calibration has the highest RMSE value for all elements, while the other two calibrations have lower and comparable RMSE values to each other.

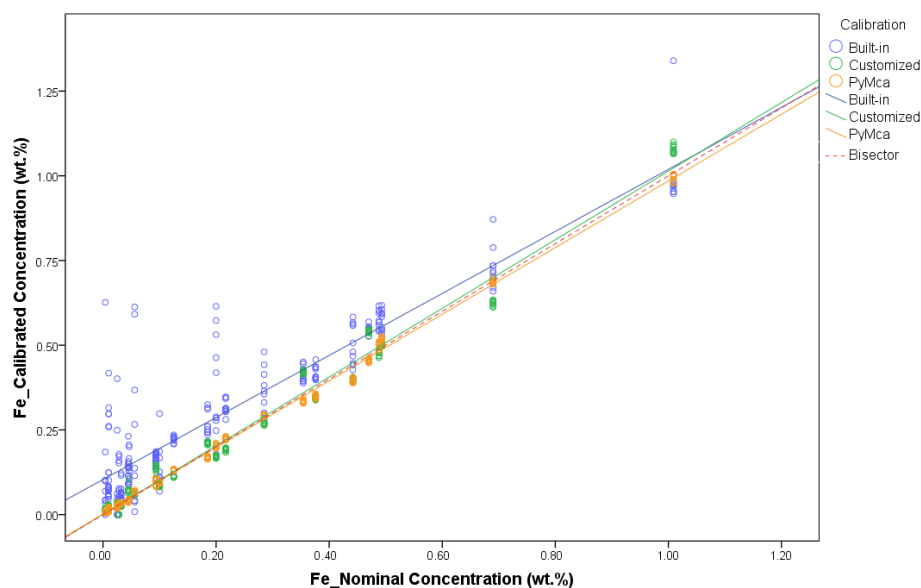


Figure 4. Linear Regression Analysis on Fe and comparison of 3 calibration procedures.

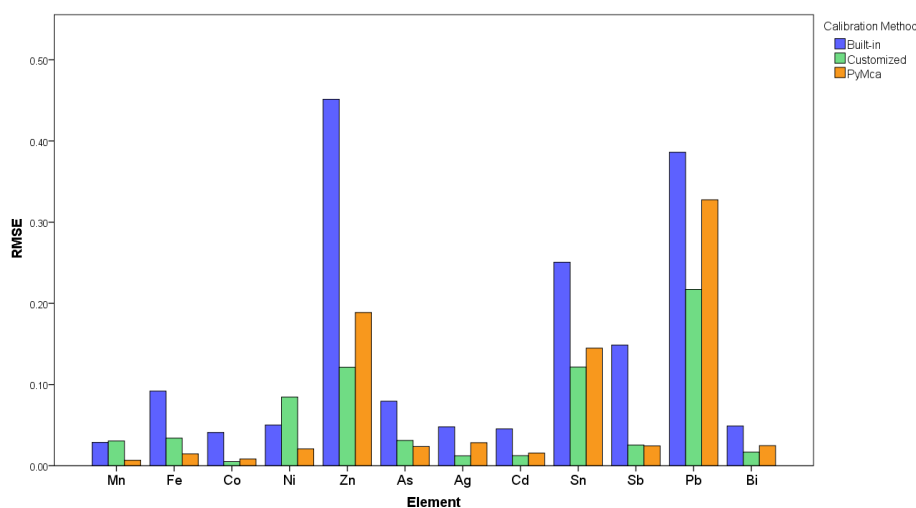


Figure 5. RMSE values obtained for all elements present in copper-based alloys.

### 3. Discussion

As highlighted by Figures 2 and 3, the poor fit of the built-in calibration for Tin (Sn) and Antimony (Sb) high-Z elements in Tracer 5g can be attributed to the fixed “copper alloy” set-up characterized by a low voltage of 15 kV (as shown in Table 2). Due to this low voltage, only the L-lines of Sn and Sb were utilized for the quantitative analysis. However, the family of L lines of these two elements are in the same energy range, leading to overlapping and making it difficult to obtain accurate quantitative results. Instead for the other two calibration approaches, offline PyMca and Bruker Customized Calibrations, we used a higher voltage to excite the K-lines of Ag, Sn, and Sb. This optimization resulted in improved calibration accuracy, as shown by the results.

**Table 2.** List of 26 certified reference materials (CRMs).

Reference Material	Supplier	Mass Weight in %																					
		Mg	Al	Si	P	S	Cr	Mn	Fe	Co	Ni	Cu	Zn	As	Se	Ag	Cd	Sn	Sb	Te	Au	Pb	Bi
1116	Department of Commerce Malcolm Baldrige Secretary (Washington, DC, USA)	-	-	-	0.008	-	-	-	0.046	-	0.048	90.37	9.44	-	-	-	-	0.044	-	-	-	0.042	-
31X 7835.8-B4	MBH Analytical LTD (London, EN, UK)	-	0.219	-	0.154	-	-	0.010	0.045	0.313	0.157	72.7	21.55	0.151	-	0.549	0.094	0.451	0.110	0.101	-	3.22	0.101
31X 7835.9-B2		-	0.120	0.047	0.062	0.020	-	0.005	0.185	0.115	0.195	76.58	16.20	0.098	0.300	2.00	0.058	1.61	0.460	-	-	1.05	0.900
31X TB5-B6		-	0.071	0.111	0.025	-	0.003	0.283	0.094	0.020	0.106	61.49	35.62	0.396	-	0.216	0.490	0.129	0.229	-	-	0.575	0.292
32X LB10-G1		-	-	-	0.003	0.010	-	-	-	0.084	0.69	77.40	0.110	0.165	-	0.070	-	8.25	0.600	0.010	-	12.5	0.092
32X LB14-G1		-	0.001	0.001	0.058	0.018	-	0.001	0.009	0.089	0.254	77.01	0.586	0.050	-	0.120	-	5.63	0.075	-	-	15.42	0.720
32X LB17-A4		-	0.388	-	0.051	-	0.001	0.296	0.488	0.008	0.465	74.83	0.634	1.51	-	0.911	0.151	5.97	4.10	-	-	9.83	0.220
32X PB12-E3		0.003	0.007	0.010	0.172	0.013	-	0.011	0.032	0.014	0.221	93.29	0.546	0.087	-	-	-	5.25	0.160	-	-	0.102	0.057
32X SN5-B1		-	0.215	-	-	-	0.023	0.528	1.01	0.129	0.667	78.97	0.604	0.056	-	0.095	0.130	15.9	0.702	0.001	0.010	0.860	0.124
32X SN6-B3		-	0.059	-	-	-	0.015	0.090	0.376	0.75	0.295	85.73	2.00	0.804	-	1.01	0.024	6.78	0.304	-	0.003	1.64	0.127
33X GM20-B3		-	0.133	-	0.060	-	-	0.040	0.442	0.021	0.211	89.49	1.80	0.300	-	0.200	0.020	4.49	2.41	-	-	0.294	0.044
33X GM21-B6		-	0.175	0.022	0.068	0.064	-	-	0.690	-	0.200	78.96	4.95	0.335	0.177	0.700	0.250	4.50	1.05	-	-	7.40	0.460
33X GM4-AD1		-	0.002	0.001	0.003	0.034	-	0.001	0.093	0.001	1.48	84.02	5.90	0.023	-	0.021	-	3.02	0.057	-	-	5.27	0.044
33X RB2-A3		0.001	0.036	0.012	0.021	0.078	0.002	0.003	0.493	0.035	0.255	82.67	9.14	0.021	-	0.003	-	3.19	0.019	-	-	3.85	0.101
B14	Centre Technique des Industries de la Fonderie (Sevres, FR)	-	-	0.110	0.700	0.021	-	0.014	0.125	-	0.302	86.80	0.175	0.039	-	-	-	11.10	0.072	-	-	0.520	-
B21		-	0.130	-	0.004	0.047	-	-	0.285	-	1.21	83.05	6.17	-	-	-	-	5.13	0.180	-	-	3.79	-
B3		-	0.130	0.062	0.480	0.046	-	0.194	0.217	-	1.53	80.25	2.26	-	-	-	-	12.96	0.204	-	-	1.65	-
BS836A-2	Brammer Standard Company (Houston, TX, USA)	-	0.002	0.002	0.083	0.042	-	0.001	0.025	-	0.460	84.70	4.55	0.008	-	0.023	-	4.58	0.068	-	-	5.32	-
CURM No.42.23-2	Bureau of Analysed Samples Ltd. (Middlesbrough, EN, UK)	-	0.008	0.015	0.128	0.045	-	0.019	0.354	-	0.168	74.36	22.13	0.168	-	-	-	1.63	0.356	-	-	0.575	0.034
CURM No.54.01-4		0.008	0.040	0.039	0.053	0.023	-	0.158	0.028	-	0.348	95.42	0.346	0.044	-	-	-	3.17	0.070	-	-	0.307	-
SS 551	British Chemical Standard (Warwickshire, EN, UK)	-	0.052	0.018	1.01	-	-	-	0.200	-	0.760	87.40	0.740	-	-	-	-	8.92	-	-	-	0.790	-
SS 552		-	0.023	0.019	0.770	-	-	-	0.100	-	0.560	87.70	0.350	-	-	-	-	9.78	-	-	-	0.630	-
SS 553		-	0.017	0.022	0.680	-	-	-	0.056	-	0.440	87.00	0.490	-	-	-	-	10.8	-	-	-	0.470	-
SS 555		-	0.005	0.036	0.180	-	-	-	0.010	-	0.110	87.10	0.160	-	-	-	-	12.1	-	-	-	0.240	-
SS 556		-	0.005	0.005	0.100	-	-	-	0.004	-	0.014	86.40	0.090	-	-	-	-	13.2	-	-	-	0.160	-
UZS60	Centre de développement des industries de mise en forme del materiaux (Sevres, FR)	-	-	3.72	0.070	-	-	-	0.470	-	0.490	78.98	15.3	-	-	-	-	0.40	-	-	-	0.570	-

Regardless of the voltage value, there are cases where overlapping is unavoidable in Low-Z elements. A typical example is Iron (Fe) (Figure 4). The fact that we have smaller deviations in the calibrated Iron concentrations in both Off-Line PyMca and Customized Bruker relative to the Built-in Calibration is because we were able to optimize the results for that element separately during the calibration procedure. Both external PyMca and internal Easycal software (PyMca version 5.9.2. and the Bruker EasyCal software) enable the user to highlight a particular element contribution in order to improve its quantitative results by inter-element corrections. For example, in the calibration procedure to avoid the overlapping between the Lead and Arsenic elements, we choose to use in the calibration Pb Lb1 to avoid the overlap of As Ka1, and for the calibration of As we choose As Kb1. Unlike this, the Bruker Built-in fixed set-up does not allow the improvement of the individual element, which means that the final results are directly obtained. In Figure 4 and Table 1, the results clearly indicate a difference in accuracy. The R squared value for the Iron (Fe) element in the Bruker Built-in Calibration is 0.86, while the other two calibrations have an R squared value of 0.99 (PyMca) and 0.98 (Customized Bruker) (Table 1). The lower accuracy of elemental quantitative results observed in the Built-in Calibration across all elements present in copper-based alloys (Figure 5) can be explained by the fact that general-purpose standards were used in the calibration procedure rather than specific ones having a similar composition to cultural heritage copper alloys.

Non-specific and modern reference materials do not provide a complete representation of the minor elements that are commonly present as impurities in copper alloys found in historical artefacts. In fact, these elements are either not present or found in lower levels than those typically observed in copper archaeological artefacts, especially for elements such as Fe, As, Bi, Ag, and Sb. This highlights the importance of using appropriate standards for the XRF analysis of historical copper alloys [27]. For this reason, for the other two calibrations, a set of certified and compositionally significant standards, as they represented heritage copper-based artefacts, was utilized.

## 4. Materials and Methods

### 4.1. Reference Materials

A group of 26 certified reference materials (CRMs), compositionally significant in heritage copper-based artefacts, was used for the experiments (see Table 2). Part of the references are from the Charm Set [27], while the others were added to expand the composition range, similar to that of ancient copper alloys. For each standard, the uncertainty values were generated from the 95% confidence interval and in our calibration certified values of the following elements were used: Mn, Fe, Co, Ni, Zn, As, Ag, Cd, Sn, Sb, Pb, Bi. The majority of standards were in the shape of a disk, with a diameter ranging from 28 to 55 mm and a thickness ranging from 5 to 17 mm. Moreover, the standards were not constituted by multilayers but had the same composition, and the single suppliers guaranteed their homogeneity through statistical assessment and testing. Based on the article of Porcinai et al. [29], the subsurface layers that provide 99% of the maximum fluorescent intensity for the  $K\alpha$ -line of Antimony (the most energetic line fluorescence present in the copper material) have a thickness of about 210 microns. Therefore, we can assume that the measurements are conducted under infinite thickness conditions, considering that the size of the reference is several millimeters. For each calibration procedure, 10 series of measurements were performed on the whole group of standards, so the data set for each method separately was made of 260 records.

### 4.2. Calibration Procedures

#### 4.2.1. Off-Line PyMca Calibration

For the first calibration procedure, we used the Fundamental Parameters software PyMca [28]. It is a user-friendly program for X-ray Fluorescence Analysis, which has been developed at the European Synchrotron Radiation Facility, so it is an independent software from the instrument manufacturer used in this work. Before starting the experiments,

a study was carried out to find the optimal voltage, current, and primary filtration for Tracer 5g. Then, we performed 10 series of measurements on reference materials and collected the different spectra to process and quantify them off-line with PyMca. Once the quantification had been performed, the spectra were subjected to calibration by Weighted Linear Regression (WLS) method. Heginbotham et al. [30] have described a protocol for quantification of heritage copper alloys by ED-XRF with the use of PyMca. However, we followed a modified method described by a previous study from Konstantakopoulou et al. [31], where the optimal conditions for Tracer 5g are reported, as well as the detailed steps for the calibration procedure.

#### 4.2.2. Customized Bruker Calibration

Bruker provides software EasyCal and a detailed procedure for creating customized calibrations in Tracer 5g based on the empirical coefficients method. According to the procedure suggested by the manufacturer, before the start of the experiments it was necessary to choose standards and define the optimal excitation parameters. For this purpose, we used the same working conditions as those of Off-Line PyMca Calibration. With the use of EasyCal toolbox, we were able to set up the calibration curves but also to improve them for every element separately regarding several parameters such as line overlaps, standard deviation, etc.

After completing all required steps, the Customized Bruker calibration was installed in Tracer 5g and it was ready to be used. We performed 10 series of measurements on reference materials and the quantitative results corresponding to the customized calibrated values were displayed in real time on the device screen.

#### 4.2.3. Bruker Built-In Calibration

There are several built-in calibrations in Tracer 5g corresponding to a variety of materials. These calibrations are based in empirical coefficients, are pre-installed by Bruker, and provided through the remote control of the instrument. For this study, we chose the one named "Copper alloys".

Compared to the previous two methods, Bruker Built-in Calibration has predetermined working conditions for Tracer 5g, which cannot be changed and at the same time the operator has no access to the details of the calibration procedure that has been performed by the manufacturer. Having these limitations, the only step we followed in this case was to perform 10 series of measurements on the reference materials. The elemental quantitative results were provided directly on display without requiring further processing.

### 4.3. Statistical Techniques

To compare the quantitative results obtained from the 3 different calibration procedures, we performed Linear Regression Analysis, using the nominal elemental concentration as the independent variable and the calibrated one as the dependent variable. Determining the R squared ( $R^2$ ) for the three different calibrations is a direct and reliable way to predict the most appropriate model for each element. As a measure of accuracy, we used the Root Mean Squared Error (RMSE), which is the standard deviation of the Linear Regression Residuals.

### 4.4. Instrumentation

This work considers the commercial Hand-Held XRF device "Bruker Tracer 5g". It has a Rhodium target X-ray source with a maximum high voltage of 50 kV and 4 W maximum power consumption but has automatic limitations on the tube current depending on the high voltage. Moreover, Tracer 5g has an SDD detector, while it is provided with 2 collimators (3 and 8 mm) and 4 filters.

In all calibrations, a collimator with 3 mm beam spot size was selected. This was deemed necessary as in copper-based artefacts there is inhomogeneity due to the patina. The working conditions of each calibration procedure are summarized in Table 3.

**Table 3.** Bruker Tracer 5g working conditions of each calibration procedure.

Calibration Procedure	Voltage (kV)	Current ( $\mu$ A)	Primary Filtration	Measuring Time (s)
Off-Line PyMca	49	39.3	Al (300 $\mu$ m) and Ti (25 $\mu$ m)	30
Customized Bruker	49	39.3	Al (300 $\mu$ m) and Ti (25 $\mu$ m)	30
Bruker Built-in	15	23.2	-	30

## 5. Conclusions

We have observed that the quantitative data obtained through the Built-in Bruker Calibration for “Copper alloy” shows a significant deviation from the nominal values, indicating poor performance. We have also shown that customized Bruker and PyMca Calibrations provide more accurate results for the detection of both high- and low-Z elements. These calibrations can be combined for quantifying copper-based manufactures. The customized Bruker Calibration is helpful during field acquisition and immediately provides quantitative results, while the PyMca Calibration can be used for more detailed spectrum processing. Therefore, selecting similar reference materials to copper archaeological artefacts, performing the correct set-up measurements, and adopting an assurance calibration can help obtain XRF quantitative reliable data. By using the approach described here to evaluate quantitative XRF data in copper-based artefacts using Hand-Held XRF devices, we can avoid a simplistic automatic use of the device as a “black box” and prevent inconsistencies in the quantitative data.

**Author Contributions:** Conceptualization, E.K., A.C.M. and M.F.; methodology, E.K., A.C.M. and M.F.; software, E.K. and A.C.M.; validation, E.K., A.C.M. and M.F.; formal analysis, E.K.; investigation, E.K. and A.C.M.; resources, E.K. and A.C.M.; data curation, E.K. and M.F.; writing—original draft preparation, E.K.; writing—review and editing, E.K., A.C.M. and L.L.; visualization, M.F. and L.L.; supervision, A.C.M., L.L. and M.F.; All authors have read and agreed to the published version of the manuscript.

**Funding:** This research received no external funding.

**Data Availability Statement:** The data presented in this study are available and will be given upon reasonable demand from the corresponding author.

**Acknowledgments:** The authors are grateful for the Erasmus+ program which supported the traineeship on analyzing heritage metals using high-energy XRF spectrometry at the Institute of Heritage Science of the National Research Council in Rome. Moreover, the authors wish to thank the Opificio delle Pietre Dure (OPD) (Florence, Italy), and in particular Simone Porcinai, for kindly providing us with the reference materials.

**Conflicts of Interest:** The authors declare no conflicts of interest.

## References

- Shackley, M.S. An Introduction to X-Ray Fluorescence (XRF) Analysis in Archaeology. In *X-ray Fluorescence Spectrometry (XRF) in Geoarchaeology*; Shackley, M.S., Ed.; Springer: New York, NY, USA, 2011; pp. 7–44; ISBN 978-1-4419-6885-2.
- Liritzis, I.; Zacharias, N. Portable XRF of Archaeological Artifacts: Current Research, Potentials and Limitations. In *X-ray Fluorescence Spectrometry (XRF) in Geoarchaeology*; Shackley, M.S., Ed.; Springer: New York, NY, USA, 2011; pp. 109–142; ISBN 978-1-4419-6885-2.
- Analytical Methods Committee AMCTB No. 108. Hand-Held X-ray Fluorescence Analysis of Archaeological Artefacts: Challenges, Advantages and Limitations. *Anal. Methods* **2021**, *13*, 3731–3734. [[CrossRef](#)]
- Piorek, S. Handheld X-ray Fluorescence (HHXRF). In *Portable Spectroscopy and Spectrometry*; Crocombe, R., Leary, P., Kammrath, B., Eds.; Wiley: Hoboken, NJ, USA, 2021; pp. 423–453; ISBN 978-1-119-83557-8.
- Ferretti, M. The Investigation of Ancient Metal Artefacts by Portable X-ray Fluorescence Devices. *J. Anal. At. Spectrom.* **2014**, *29*, 1753–1766. [[CrossRef](#)]
- Karydas, A.G. Application of a Portable XRF Spectrometer for the Non-Invasive analysis of Museum Metal Artefacts. *Ann. Di Chim.* **2007**, *97*, 419–432. [[CrossRef](#)]
- Charalambous, A.; Kassianidou, V.; Pappasavvas, G. A Compositional Study of Cypriot Bronzes Dating to the Early Iron Age Using Portable X-ray Fluorescence Spectrometry (pXRF). *J. Archaeol. Sci.* **2014**, *46*, 205–216. [[CrossRef](#)]

8. Vianello, A.; Tykot, R.H. Investigating Technological Changes in Copper-Based Metals Using Portable XRF Analysis. A Case Study in Sicily. *Open Archaeol.* **2017**, *3*, 392–408. [[CrossRef](#)]
9. Colacicchi Alessandri, O.; Caruso, G.; Orazi, N.; Ferretti, M. A Technical Examination of the Great Bronzes of the Museo Nazionale Romano. *Stud. Conserv.* **2023**, *68*, 326–342. [[CrossRef](#)]
10. Ferrence, S.; Giunliamair, A. Bronze Age Metal Objects from East Crete, Greece. *ISIJ Int.* **2014**, *54*, 1139–1146. [[CrossRef](#)]
11. Fernandes, R.; Van Os, B.J.; Huisman, H.D. The Use of Hand-Held XRF for Investigating the Composition and Corrosion of Roman Copper-Alloyed Artefacts. *Herit. Sci.* **2013**, *1*, 30. [[CrossRef](#)]
12. Nicholas, M.; Manti, P. Testing the Applicability of Handheld Portable XRF to the Characterisation of Archaeological Copper Alloys. In Proceedings of the ICOM-CC 17th Triennial Conference Preprints, Melbourne, Australia, 15–19 September 2014; p. 13.
13. Markowicz, A. An Overview of Quantification Methods in Energy-Dispersive X-ray Fluorescence Analysis. *Pramana—J. Phys.* **2011**, *76*, 321–329. [[CrossRef](#)]
14. Beckhoff, B.; Kanngießer, B.; Langhoff, N.; Wedell, R.; Wolff, H. *Handbook of Practical X-ray Fluorescence Analysis*; Springer: Berlin/Heidelberg, Germany, 2006; ISBN 978-3-540-28603-5.
15. Sitko, R. Quantitative X-ray Fluorescence Analysis of Samples of Less than ‘Infinite Thickness’: Difficulties and Possibilities. *Spectrochim. Acta Part B At. Spectrosc.* **2009**, *64*, 1161–1172. [[CrossRef](#)]
16. Van Grieken, R.; Markowicz, A. *Handbook of X-ray Spectrometry*; CRC Press: Boca Raton, FL, USA, 2001; ISBN 978-0-429-20827-0.
17. Andermann, G.; Kemp, J.W. Scattered X-rays as Internal Standards in X-ray Emission Spectroscopy. *Anal. Chem.* **1958**, *30*, 1306–1309. [[CrossRef](#)]
18. Lucas-Tooth, H.J.; Price, B.J. A Mathematical Method for the Investigation of Inter-element Effects in X-ray Fluorescence Analysis. *Metallurgia* **1961**, *64*, 149–161.
19. Lucas-Tooth, J.; Pyne, C. The Accurate Determination of Major Constituents by X-ray Fluorescent Analysis in the Presence of Large Inter-element Effects. *Adv. X-ray Anal.* **1963**, *7*, 523–541. [[CrossRef](#)]
20. Sherman, J. The Theoretical Derivation of Fluorescent X-ray Intensities from Mixtures. *Spectrochim. Acta* **1955**, *7*, 283–306. [[CrossRef](#)]
21. Shiraiwa, T.; Fujino, N. Theoretical Calculation of Fluorescent X-ray Intensities in Fluorescent X-ray Spectrochemical Analysis. *Jpn. J. Appl. Phys.* **1966**, *5*, 886. [[CrossRef](#)]
22. Sitko, R.; Zawisz, B. Quantification in X-ray Fluorescence Spectrometry. In *X-ray Spectroscopy*; Sharma, S.K., Ed.; InTech: London, UK, 2012; ISBN 978-953-307-967-7.
23. Elam, W.T.; Shen, R.B.; Scraggs, B.; Nicolosi, J. Accuracy of Standardless FP Analysis of Bulk and Thin Film Samples Using a New Atomic Database. *Adv. X-ray Anal.* **2004**, *47*, 104–109.
24. Mantler, M.; Kawahara, N. How Accurate Are Modern Fundamental Parameter Methods? *Rigaku J.* **2004**, *21*, 17–25.
25. Sitko, R. Influence of X-ray Tube Spectral Distribution on Uncertainty of Calculated Fluorescent Radiation Intensity. *Spectrochim. Acta Part B At. Spectrosc.* **2007**, *62*, 777–786. [[CrossRef](#)]
26. Martindale Johnson, L.R.; Ferguson, J.R.; Freund, K.P.; Drake, L.; Duke, D. Evaluating Obsidian Calibration Sets with Portable X-ray Fluorescence (ED-XRF) Instruments. *J. Archaeol. Sci. Rep.* **2021**, *39*, 103126. [[CrossRef](#)]
27. Heginbotham, A.; Bassett, J.; Bourgarit, D.; Eveleigh, C.; Glinzman, L.; Hook, D.; Smith, D.; Speakman, R.J.; Shugar, A.; Van Langh, R. The Copper CHARM Set: A New Set of Certified Reference Materials for the Standardization of Quantitative X-ray Fluorescence Analysis of Heritage Copper Alloys\*: The Copper CHARM Set. *Archaeometry* **2015**, *57*, 856–868. [[CrossRef](#)]
28. Solé, V.A.; Papillon, E.; Cotte, M.; Walter, P.; Susini, J. A Multiplatform Code for the Analysis of Energy-Dispersive X-ray Fluorescence Spectra. *Spectrochim. Acta Part B At. Spectrosc.* **2007**, *62*, 63–68. [[CrossRef](#)]
29. Porcinai, S.; Cagnini, A.; Galeotti, M.; Ferretti, M. Quantitative Analysis of Copper Alloys by Means of Portable X-ray Fluorescence: A Comparison between Analysis of Shavings and Surfaces. *Spectrochim. Acta Part B At. Spectrosc.* **2023**, *210*, 106808. [[CrossRef](#)]
30. Heginbotham, A.; Solé, V.A. CHARMed PyMca, Part I: A Protocol for Improved Inter-laboratory Reproducibility in the Quantitative ED-XRF Analysis of Copper Alloys. *Archaeometry* **2017**, *59*, 714–730. [[CrossRef](#)]
31. Konstantakopoulou, E.; Casanova Municchia, A.; Ferretti, R.; Porcinai, S.; Ferretti, M. Quantitative Criteria to Configure and Characterise Portable X-ray Fluorescence Spectrometers. In Proceedings of the 2023 IMEKO TC-4 International Conference on Metrology for Archaeology and Cultural Heritage, Rome, Italy, 19–21 October 2023; pp. 704–708.

**Disclaimer/Publisher’s Note:** The statements, opinions and data contained in all publications are solely those of the individual author(s) and contributor(s) and not of MDPI and/or the editor(s). MDPI and/or the editor(s) disclaim responsibility for any injury to people or property resulting from any ideas, methods, instructions or products referred to in the content.